Materials Research Express

PAPER

Martensitic transformation in free-standing Cu-Al-Ni thin films with micrometric grain size

To cite this article: M Morán *et al* 2019 *Mater. Res. Express* **6** 096556

Materials Research Express

PAPER

Martensitic transformation in free-standing Cu-Al-Ni thin films with micrometric grain size

RECEIVED
9 April 2019

REVISED
10 June 2019

ACCEPTED FOR PUBLICATION
5 July 2019

PUBLISHED
12 July 2019

M Morán[1,2], A M Condó[1,2], S Bengio[1], F Soldera[3], M Sirena[1,2] and N Haberkorn[1,2]

[1] Comisión Nacional de Energía Atómica and Consejo Nacional de Investigaciones Científicas y Técnicas, Centro Atómico Bariloche, Av. Bustillo 9500, 8400 San Carlos de Bariloche, Argentina
[2] Instituto Balseiro, U. Nacional de Cuyo, Bustillo 9500. S. C. de Bariloche. Argentina
[3] Department of Materials Science & Engineering, Saarland University, D-66123 Saarbrücken, Germany

E-mail: mjmoran@cab.cnea.gov.ar

Keywords: thin films, sputtering, shape memory alloys

Abstract

The martensitic transformation of polycrystalline thin films based on shape memory alloys is usually affected by the average grain size and by the thickness. We have carried out a study of the temperature driven martensitic transformation in micrometric grain size Cu-Al-Ni films with 18R structure. Thin films with a thickness of 6 μm were grown by sputtering on highly oriented pyrolytic graphite HOPG (0001) substrate at 873 K. After that, the samples were peeled-off from the substrate and annealed at 1123 K for 30 min. The observed microstructure shows an average grain size of 3.7 ($\pm$ 0.2) μm. The martensitic start temperature (M_s) for different films ranges from 170 K to 370 K due to small changes in the chemical concentration. The influence of surface oxides and changes in the atomic order produced by post-quench aging treatments is analyzed. The results show that while surface passivation has a weak influence, changes in the atomic order increase M_s without impacting significantly on the hysteresis. Comparison with previous results of nanometric and micrometric grain size samples reveals that the barriers for the transformation are mainly given by plastic deformation at grain boundaries.

Introduction

Understanding the mechanisms that affect martensitic transformations in low dimensional systems is technologically relevant for the development of micro-actuators [1–3]. The driving force for the thermally induced martensitic transformation is given by the chemical free energy ($\Delta G^{chem} = \Delta H - T\Delta S$; where ΔH is the enthalpy and ΔS the entropy). The barriers (which determine the hysteresis) are given by the stored elastic energy and by the energy dissipated by the frictional forces [4]. In low dimensional systems, such as thin films, and nano- and microwires, the barriers are strongly affected by surface quality, the surface/volume ratio and grain boundaries [5–10].

Cu-based alloys are particularly useful for mechanical actuators due to low-cost and the possibility of tuning the martensitic starting temperature M_s, which ranges from tens of Kelvins to 470 K (highly dependent on chemical composition) [11, 12]. Cu-based alloys are usually non-magnetic being the martensitic transformation no sensitive to the magnetic field [13]. The Cu-Al-Ni system is promising for the design of nano- and micro-systems. For instance, thin films and nanopillars display the shape memory effect [14, 15] and super-elasticity [3], respectively. Cu-Al-Ni thin films with nanometric grain size usually show a martensitic transformation with hysteresis (Δh) larger than observed in the bulk ($\approx$10 K) [14–17]. For example, thin films with grain sizes $D \approx 150$ nm and $D \approx 200$–500 nm display $\Delta h \approx 45$ K and ≈ 35 K, respectively [14, 15]. It is important to note that there are no reports on the martensitic transformation of Cu-Al-Ni thin films with micrometric grain size. The study of the properties of shape memory thin films with micrometric grain size is relevant for understanding the role of other mechanisms such as surface passivation (related to the presence of oxides) [8] and austenitic order (which can be modified by thermal annealing at low temperatures) [12].

In this study, we report martensitic transformations in 6 μm thick Cu-Al-Ni thin films with 18R martensitic structure and average grain size $\hat{D} \approx 3.7\ (\pm 0.2)\ \mu$m. The present study extends our previous findings on the martensitic transformation of thin films with nanometric grain sizes [14–16]. The films were obtained in two successive steps. First, a film was grown on highly oriented pyrolytic graphite HOPG (0001) at 873 K (cooling-down *in situ* without quench). After this the film was peeled off from the substrate and annealed at 1123 K. Austenitic phase [free of α (Cu) and γ_2 (Cu_9Al_4) equilibrium phases] was obtained after fast quenching in an ice-water mixture [12]. The contribution of the microstructure, surface oxides and the influence of changes in the austenitic order (induced by thermal annealing) on the resulting temperature driven martensitic transformation are analyzed in the following.

Experimental procedure

The Cu-Al-Ni films were grown by DC sputtering on HOPG (0001) at 870 K. The target for sputtering was prepared from a high purity alloy of Cu–27.35 at.% Al–5.45 at.% Ni melted in an induction furnace under Ar atmosphere ($M_S = 240$ K and $\Delta h \approx 10$ K). The deposition parameters used were: an atmosphere of 10 mtorr of argon, an applied power of 50 watts and a distance target/substrate of 7 cm. The growth rate was ~ 50 nm min^{-1}. After growth, the films were cooled down in vacuum by turning-off the heater, which results in a microstructure with the coexistence of austenite $L2_1$, and α (Cu) and γ_2 (Cu_9Al_4) equilibrium phases. The films, with typical size of 1 cm^2, were peeled off from the substrate with glue tape (the glue was later removed with organic solvents) and were encapsulated in quartz tubes under an atmosphere of argon (inside a tantalum envelope). Thermal annealing was performed at 1123 K for 30 min. This temperature was selected considering the equilibrium phase diagram for Cu-Al-Ni [18]. After the annealing process, the samples were fast quenched in an ice-water mixture.

The microstructure of the films was studied by transmission electron microscopy (TEM) and energy-dispersive x-ray spectroscopy (EDS) using two different microscopes (CM200 UT and FEI Tecnai F20 UT). Plan-view TEM specimens were made by ion-milling (Ar^+: 3 keV and angle 7°). Cross-section TEM specimens were prepared by using a focused ion beam (FIB) / SEM dual beam FEI Helios NanoLab 600 equipped with an Omniprobe 100 micromanipulator. The crystalline properties of the films were characterized by a PANalytical Empyrean x-ray diffractometer using Cu-Kα radiation with an accelerating voltage of 40 kV and a current of 30 mA. Surface composition was investigated by x-ray photoelectron spectroscopy (XPS) using a standard Al/Mg twin-anode x-ray source and a hemispherical electrostatic electron energy analyzer. The samples were measured in high-vacuum conditions with a base pressure of 10^{-9} Torr. The Fermi level of adventitious carbon was used as the reference to calibrate the binding-energy (BE) scale. Surface cleaning was performed with Ar^+ sputtering (3 keV) at a rate of ≈ 1.5 nm min^{-1}. The martensitic transformation was characterized by electrical transport using a conventional four-probe geometry.

Results and discussion

The results are divided in three different sections. The goal is to understand the influence of different mechanisms (grain boundaries, surface passivation and atomic order) on the resulting temperature driven martensitic transformation. The first refers to the characterization of microstructure and the martensitic transformation of Cu-Al-Ni thin films. We selected samples with M_s of 178 and 348 K with 18R martensite structure. The comparison between both extremes of M_s discards the influence of slight changes in composition as a source of increment in the hysteresis for $L2_1 \rightarrow$ 18R transformation. The differences in M_s are related to small modifications in the chemical concentration (<1 wt.% Al [12]). The M_s value is affected by the relative position between the substrate and the target [14]. The second section refers to the analysis of the chemical composition of surface oxides and their influence on the martensitic transformation [8]. The third section analyses the impact of the $L2_1$ order on the temperature driven transformation of micrometric grain size Cu-Al-Ni thin films.

Microstructure and temperature driven martensitic transformation

The results correspond to samples produced by thermal annealing and quenching in ice-water. The films were cut in pieces of 0.1 cm × 0.4 cm. Figures 1(a), (b) show the temperature dependence of the normalized resistance for two Cu-Al-Ni films. The M_s values are of 178 and 348 K, respectively. The Δh values are of $\approx$ 28 K and $\approx$ 30 K, respectively. The x-ray diffraction patterns show that at room temperature the films are in the austenitic phase and martensite 18R, respectively (see figures 1(c), (d)). The austenite phase displays a texture with $\{220\}_{L21}$ planes parallel to the plane of the films. Figures 1(e), (f) show plan-view TEM images for the respective microstructures. The films are polycrystalline with average grain size $\hat{D} \approx 3.7\ (\pm 0.2)\ \mu$m (see Figure 2).

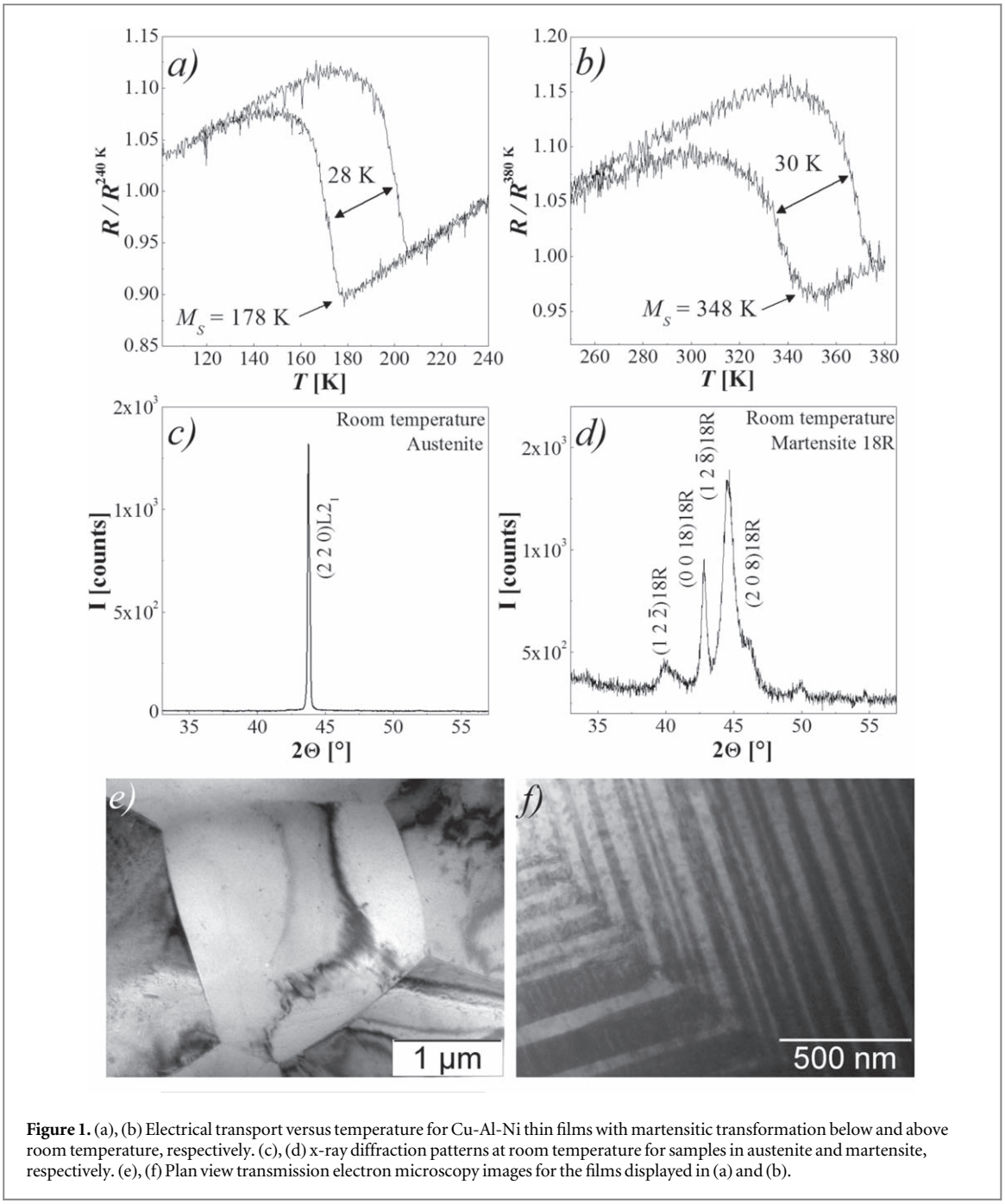

Figure 1. (a), (b) Electrical transport versus temperature for Cu-Al-Ni thin films with martensitic transformation below and above room temperature, respectively. (c), (d) x-ray diffraction patterns at room temperature for samples in austenite and martensite, respectively. (e), (f) Plan view transmission electron microscopy images for the films displayed in (a) and (b).

The chemical driving force ΔG^{chem} generated by undercooling around T_0 (related to the $\Delta S^{L21\rightarrow 18R}$) can be estimated as $\partial \Delta G/\partial T = -\Delta S$ [19] (with $\Delta S^{L21\rightarrow 18R} \approx -2 \times 10^5\ J\ K^{-1}\ m^{-3}$ [20]). For bulk specimens with large grain sizes and $(\Delta h/2) \approx 5$ K, the total energy barrier is $E^{T\text{-}bulk} = (\Delta h/2) \times \Delta S \approx 1 \times 10^6\ J\ m^{-3}$. A Δh value of ≈ 30 K corresponds to a barrier $E^{T\text{-}Film} \approx 3 \times 10^6\ J\ m^{-3}$. We then focused on understanding the reasons for the hysteresis observed in Figures 1(a), (b). The evolution of the hysteresis for polycrystalline Cu-Al-Ni with a wide range of grain sizes (3–100 μm) is analyzed in refs. [10, 17]. The Δh in bulk samples with a grain size between 3 μm and 10 μm takes values between ≈ 40 K and 25 K [15]. For $D > 3$ μm, the barrier follows a $\Delta h \propto (1/D)$ dependence, which is related to an increment of the frictional work at grain boundaries when the grain size is reduced. According to [17], accommodation of the martensite plates produces a region rich in dislocations on both sides of the grain boundaries with a thickness of ≈ 300 nm. The plastic deformation in these regions increases the hysteresis during the martensitic transformation/retransformation. To verify the presence of a similar mechanism in our films, we analyzed the microstructure of the grain boundaries in a thermally cycled Cu-Al-Ni film (the film was cycled between liquid nitrogen and room temperature several times). Figure 3 shows a TEM image where a high density of dislocations is present in a region with a thickness of ≈ 350 nm, which is in agreement with the mechanism described in [17]. The interaction of the moving interfaces with the

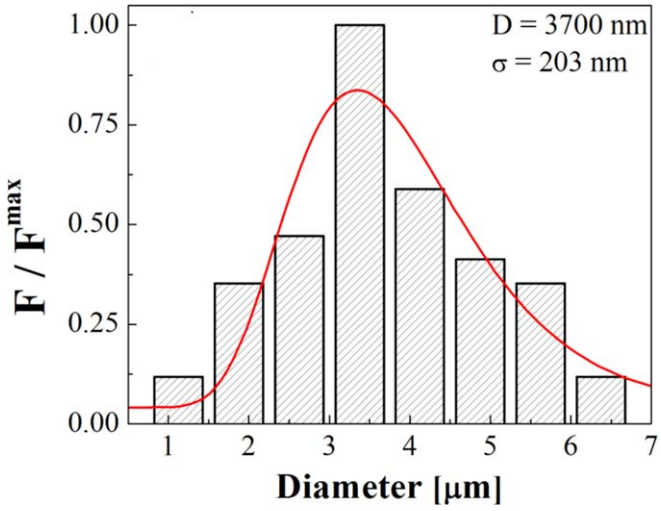

Figure 2. Histogram of the grain size distribution.

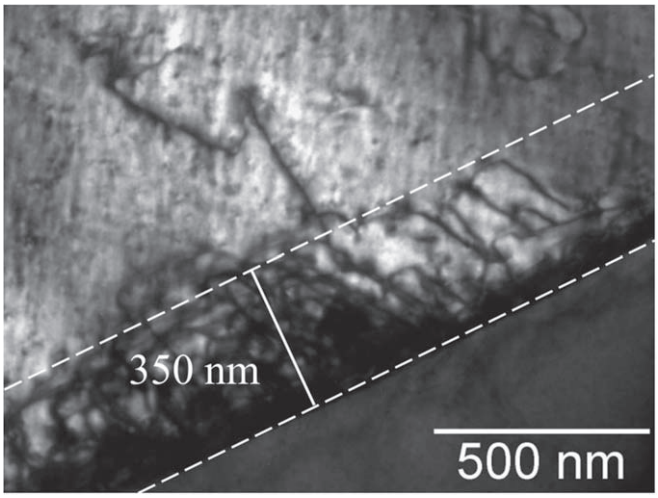

Figure 3. TEM bright field image of a Cu-Al-Ni film after several thermal cycles.

high density of dislocation zone involves energy dissipation per unit of volume (E^{dis}) that can be estimated by the following expression:

$$E^{dis} = \frac{\gamma^{dis} A}{V} \sim \frac{\gamma^{dis}}{d_m}, \quad (1)$$

where γ^{dis} is the dissipative energy per unit of area of the grain boundary ($\sim 2.6\ \mathrm{J\ m^{-2}}$) and d_m is the width of the high density of dislocations region. E^{dis} for a $d_m = 350$ nm is $\approx 7 \times 10^6\ \mathrm{J\ m^{-3}}$, in the same order of magnitude as $E^{T\text{-}Film}$.

An expected difference between films and bulk is related to surface barriers. In metallic surfaces (without oxides), the change in the surface energy (normalized by volume) produced by the martensitic transformation is $\Delta\gamma_{sf} = \gamma_{sf}^{M} - \gamma_{sf}^{A}$ (with $\Delta\gamma_{sf}$ the difference in surface energy per unit area of martensite and austenite, and multiplies the specific sample surface area A_{sf}) [6]. Surface energies of metallic materials are usually very low $\approx$ 1–3 $\mathrm{J\ m^{-2}}$ [21]. Considering $\Delta\gamma_{sf} \leqslant 1\ \mathrm{J\ m^{-2}}$ and the surface / volume ratio $\approx 2/t$, the $\Delta\gamma_{sf} A_{sf}$ contributions should be $\approx 4 \times 10^5\ \mathrm{J\ m^{-3}} \approx 2$ K in samples with $t \approx 6\ \mu$m (an order of magnitude lower than the $E^{T\text{-}Film} \approx 3 \times 10^6\ \mathrm{J\ m^{-3}}$). Although surface barriers have an influence smaller than that produced by grain boundaries, the formation of oxides and topological defects may increase its contribution [8]. Specifically, in Cu-based alloys, oxides are formed during the quench process. In the following, we analyze surface passivation and its influence in the martensitic transformation.

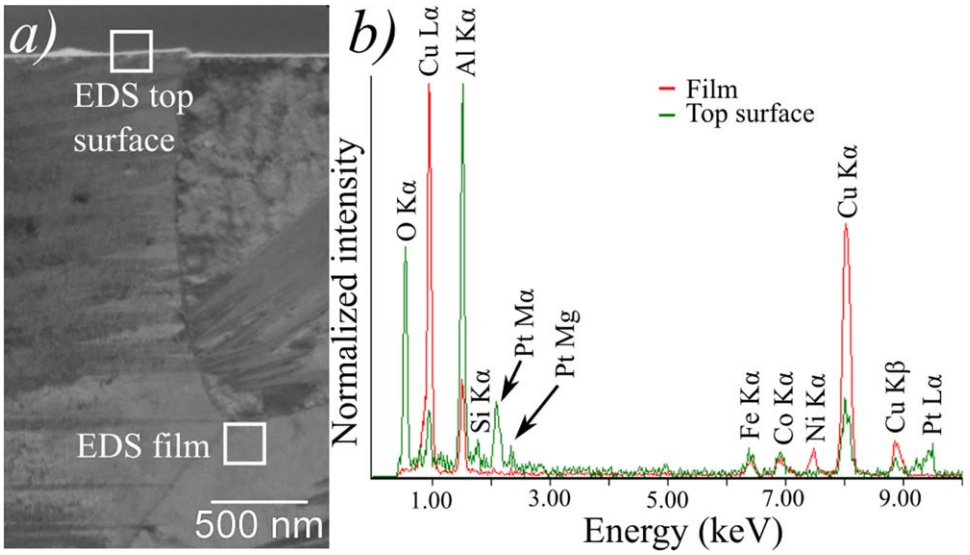

Figure 4. (a) TEM bright field cross section image of a Cu-Al-Ni film. Marks show the sites were the EDS analysis were performed. (b) EDS inside film and EDS at film surface.

Surface analysis

Figure 4(a) shows a cross-section TEM image of a Cu-Al-Ni film in the austenitic phase. The surface of the sample displays a change in the contrast that could be related to the presence of oxides. Figure 4(b) shows the EDS spectrum for the surface and the core of the films. The results show a 10 nm thick layer rich in Al_2O_3 close to the surface. The chemical composition of the surface of the samples was analyzed by XPS. In addition, a comparison between the martensitic transformation in films after and before the removal of the oxide layer is presented.

The information of elements in thin films and contamination adsorbed on the thin films can be inferred from the XPS wide scan spectra. Figure 5 shows the survey spectra obtained for the top and bottom surfaces of the film before and after removal of the oxide layer with successive steps of ion milling (composition depth profile). The spectra show components related to Cu2p, Ni2p, O1s, N1s, Ag3d (the Ag is a residue of electrical contacts), C1s, Al2s (overlapping with Cu3s) and Al2p (overlapping with Cu3p). After cleaning the surface ($\approx$ 2–3 nm in depth), the spectra show peaks corresponding to Cu2p, O1s, C1s, Al2s, and Al2p. The Al components can be attributed mainly to Al_2O_3 [22]. The spectrum at a depth of $\approx$ 15 nm shows an increment of the Cu2p and Ni2p, components and a reduction of the C1s and O1s components (in agreement with the EDS analysis). It is important to note that the components corresponding to O1s and N1s remain in the spectra at depth of $\approx$ 36 nm and 60 nm (impurities in the core of the film). Figure 6 shows the depth profiling of the Al2s and the Cu3p peaks. The spectra were fitted using a Voigt function for each peak plus a Shirley-type background. The surfaces show a majority component of Al_2O_3 with binding energy BE $=$ 120.3 eV and a minor one of metallic Al with BE $=$ 118 eV. The peak corresponding to Cu3s is observed at BE $=$ 122.5 eV. The profiles at depths above 15 nm show increments of the component corresponding to metallic Al and Cu. It is important to note that for the bottom surface the component related to Al2s shifts to lower BE, compatible with the presence of AlN, whose BE is $\approx$ 119.4eV. The presence of oxides and nitrides in the core of the film may be formed during the sputtering process (by residual impurities in the chamber).

Figure 7 shows a comparison between the temperature driven martensitic transformation of an as formed film and one with surfaces cleaned during the XPS analysis. The results show that there are no changes in the M_s and the hysteresis, indicating a negligible contribution of oxides for 6 μm thick Cu-Ni-Al thin films. Although it is outside the scope of this manuscript, it is important to mention that the insignificant contribution of the surface layers in the martensitic transformation of Cu-Al-Ni may be relevant for the application of coatings that allow making it biocompatible [23].

Annealing of Cu-Al-Ni at low temperatures

The crystalline microstructures of the martensite phases in Cu–Al–Ni can be changed with heat treatment, either by varying the quenching rate or by aging at different temperatures [24–26]. Considering that the films are quenched from 1123 K, the influence of aging at low temperatures on the microstructure and the resulting martensitic transformation was analyzed. Cu-Al-Ni films were annealed for times up to 2700 min at 423 K in air. This annealing temperature allows the relaxation of internal strain and modifies the order without precipitation

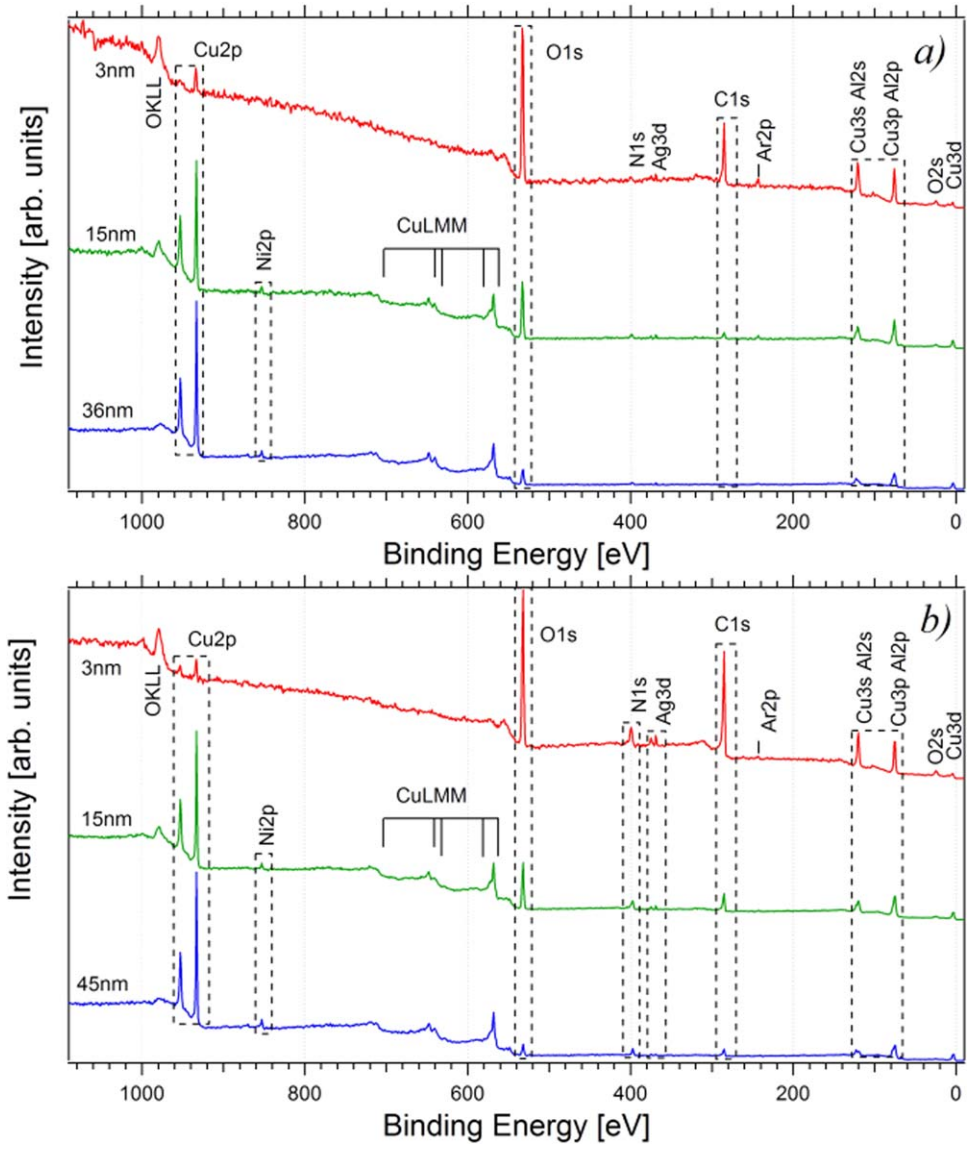

Figure 5. In-depth Al2s (overlapping with the peak Cu3s) spectra at (a) top and (b) bottom surfaces of a Cu-Al-Ni thin film, respectively. The surface was successively sputtered with Ar^+ (3 kV) and the top spectra correspond to an in-depth of 3 nm, the medium spectra to 15 nm and the bottom spectra to approximately 40 nm.

of γ_2 phase [12]. Figure 8(a) shows a summary of the results. TEM images corresponding to the initial and final microstructures are included (see figures 8(b) and (c)). The thermal annealing increases the M_s value and reduces the transformation/retransformation ranges. The hysteresis is not appreciably affected for the analyzed aging times. For instance, the M_s value is increased from 260 K to ~ 300 K after annealing for 1460 min, and the hysteresis remains in ~ 27 K. The shift in M_s could be related to an increase in the equilibrium temperature $T_0 = (M_s + A_f)/2$ (with A_f the austenitic finish temperature) produced by changes in the order of the austenite (see inset figure 8(a)) [26]. It is important to note that the initial martensitic transformation is recovered when films aged at 473 K are subjected again to heating at 1123 K and subsequently quenched again in ice-water. The recovering of the initial transformation indicates that no irreversible changes are produced during the annealing at 473 K.

Summary

We analyzed the energy barriers in the temperature driven martensitic transformation of micrometric grain size Cu-Al-Ni films with 18R structure. The main emphasis of this study is on understanding the role of the surface barrier and the atomic order on the martensitic transformation when the grain size is of the same order of magnitude as the thickness. The films display M_s between ≈ 180 K and ≈ 350 K. The average grain size is

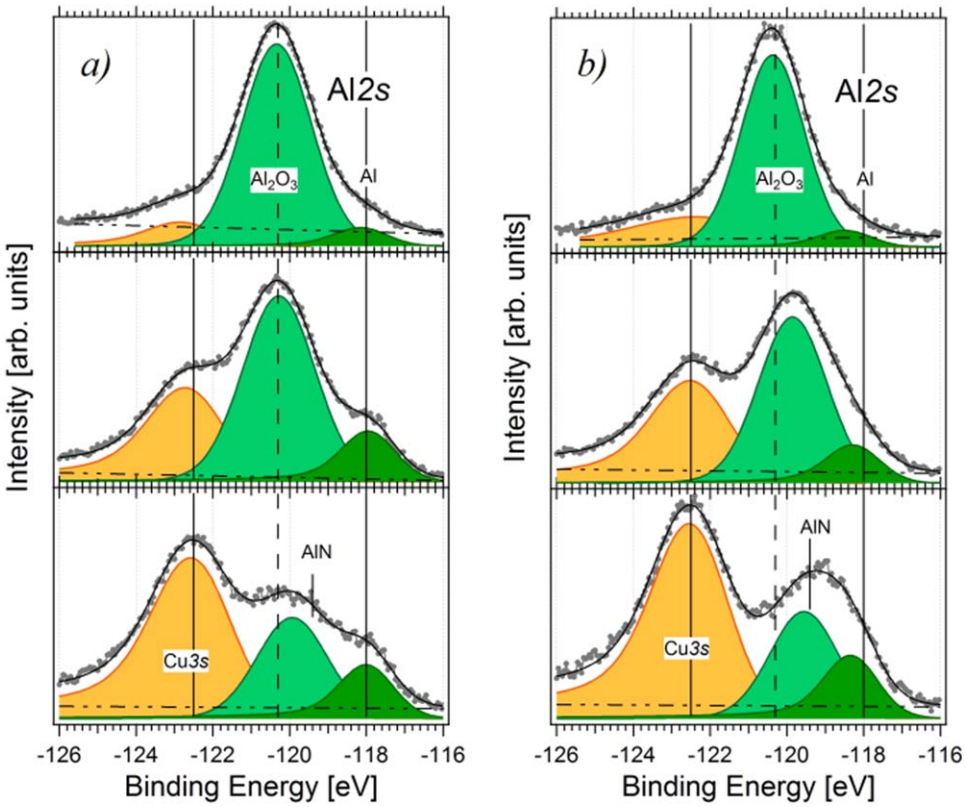

Figure 6. In-depth Al2s (overlapping with the peak Cu3s) spectra at (a) top and (b) bottom surfaces of a Cu-Al-Ni thin film.

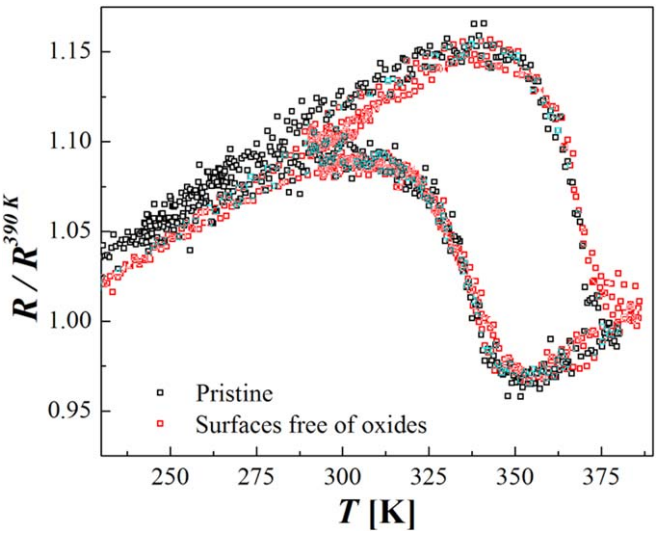

Figure 7. Electrical transport versus temperature for Cu-Al-Ni thin films after and before removal of surface oxides by argon sputtering.

$\hat{D} \approx 3.7\,(\pm 0.2)\,\mu$m. The obtained results complement previous studies in nanocrystalline Cu-Al-Ni thin films [14–16].

The results show that the hysteresis of the transformation is similar to that observed in bulk specimens with similar grain size ($E^{T\text{-}Film} \approx 3 \times 10^6\,\mathrm{J\,m^{-3}}$). The presence of a high density of dislocations at the grain boundaries indicates that in agreement with the bulk, the plastic deformation by accommodation of martensite plates contributes to increasing the barrier for the transformation [17]. Unlike films with nanometric grain sizes, the martensite plates are extended through the film thickness.

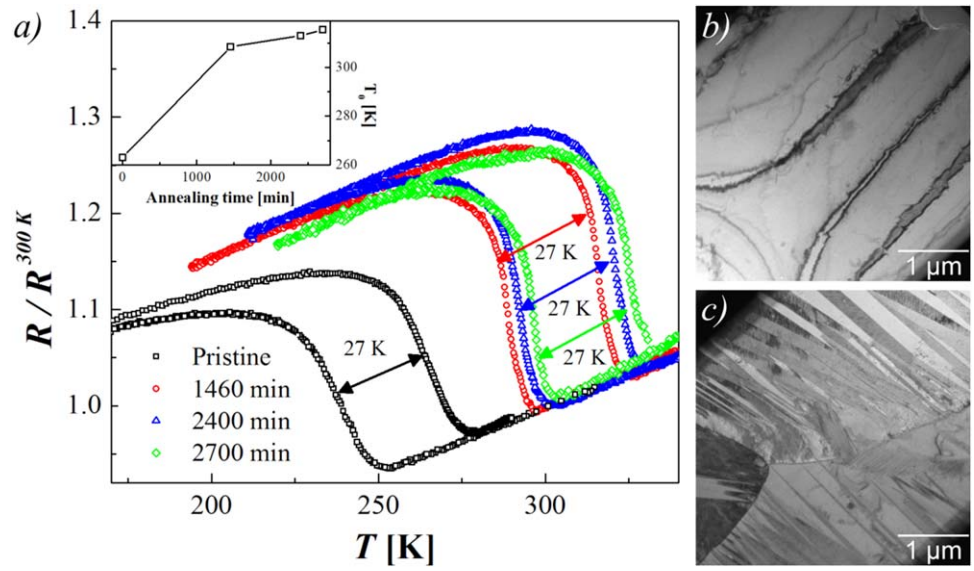

Figure 8. (a) Electrical transport versus temperature for an as-quenched film and films annealed at 473 K for 1460, 2400 and 2700 min. Inset shows the T_0 dependence with the annealing time. (b) TEM bright field cross section image of pristine film. (c) TEM bright field cross section image of the film annealed at 473 K for 2000 min. Martensite plates can be observed. The normal (n) to the substrate surface is parallel to the growing direction.

We analyzed in detail the presence of oxides at the surfaces. The films display an oxide layer with a thickness of $\approx$ 10 nm (mainly Al_2O_3). There are no differences between the martensitic transformation of as formed and surface treated films. In addition of the analysis of barriers imposed by the surface, we analyze the influence of atomic order on the resulting properties. We found that changes in the atomic order increase T_0 without modifying the barriers for the transformation (produced by grain boundaries).

The similitude in the martensitic transformation between thin films and bulk with similar microstructure suggests that the design of epitaxial structures is necessary to reduce the contribution of grain boundaries. To understand the role of the dimension and the microstructure on the resulting martensitic transformation of Cu-based alloys is necessary for their application in the development of micromechanical systems.

Acknowledgments

We would like to thank P. Troyon, M. Corte, E Aburto and M Isla. This work was supported by ANCYPT PICT 2012-0884. M M, S B, M S and N H are members of the Instituto de Nanociencia y Nanotecnología, CNEA-CONICET (Argentina).

Conflicts of interest

All other authors report no **conflicts of interest** relevant to this article.

ORCID iDs

M Morán https://orcid.org/0000-0001-9360-0723
N Haberkorn https://orcid.org/0000-0002-5261-1642

References

[1] Yuan Z, Ken G and Zhu T 2012 Atomistic characterization of pseudoelasticity and shape memory in NiTi nanopillars *Acta Mater.* **60** 6301–11
[2] Liu L, Ding X, Jun S, Suzhi L and Salje E K H 2016 Breakdown of shape memory effect in bent Cu−Al−Ni nanopillars: when twin boundaries become stacking faults *Nano Lett.* **16** 194–8
[3] San Juan J, Nó M L and Schuh C A 2012 Superelastic cycling of Cu–Al–Ni shape memory alloy micropillars *Acta Mater.* **60** 4093–106
[4] Petryk H, Stupkiewicz S and Maciejewski G 2010 Interfacial energy and dissipation in martensitic phase transformations: II. Size effects in pseudoelasticity *J. Mech. Phys. Solids* **58** 373–89
[5] Frick C P, Orso S and Arzt E 2007 Loss of pseudoelasticity in nickel-titanium sub-micron compression pillars *Acta Mater.* **55** 3845–55

[6] Chen Y and Schuh C A 2011 Size effects in shape memory alloy microwires *Acta Mater.* **59** 537–53
[7] Ueland S M and Schuh C A 2013 Transition from many domain to single domain martensite morphology in small-scale shape memory alloys *Acta Mater.* **61** 5618–25
[8] Ueland S M and Schuh C A 2014 Surface roughness-controlled superelastic hysteresis in shape memory microwires *Scr. Mater.* **82** 1–4
[9] Waitz T, Pranger W, Antretter T, Fischer F D and Karnthaler H P 2008 Competing accommodation mechanisms of the martensite in nanocrystalline NiTi shape memory alloys *Mater. Sci. Eng.* A **481–482** 479–83
[10] La Roca P, Isola L, Vermaut P and Malarria J 2015 Relationship between martensitic plate size and austenitic grain size in martensitic transformations *Appl. Phys. Lett.* **106** 221903–6
[11] Ahlers M 1986 Martensite and equilibrium phases in CuZn and CuZnAl alloys *Prog. Mater Sci.* **30** 135–86
[12] Recarte V, Perez-Saez R B, Bocanegra E H, Nó M L and San Juan J 1999 Dependence of the martensitic transformation characteristics on concentration in Cu–Al–Ni shape memory alloys *Mater. Sci. Eng.* A **273–275** 380–4
[13] Marcos J, Planes A, Mañosa L, Labarta A and Hattink B J 2002 Martensitic transition and magnetoresistance in a Cu-Al-Mn shape-memory alloy: influence of ageing *Phys. Rev.* B **66** 054428–544288
[14] Moran M J, Condo A M, Soldera F, Sirena M and Haberkorn N 2016 Martensitic transformation in freestanding and supported Cu-Al-Ni thin films obtained at low deposition temperatures *Mater. Lett.* **184** 177–80
[15] Espinoza Torres C, Condo A M, Haberkorn N, Zelaya E, Schryvers D, Guimpel J and Lovey F C 2014 Structures in textured Cu–Al–Ni shape memory thin films grown by sputtering *Mater. Charact.* **96** 256–62
[16] Moran M, Condo A M and Haberkorn N 2018 Recrystallization and martensitic transformation in nanometric grain size Cu-Al-Ni thin films grown by DC sputtering at room temperature *Mater. Charact.* **139** 446–51
[17] La Roca P, Isola L, VermautPh and Malarría J 2017 Relationship between grain size and thermal hysteresis of martensitic transformations in Cu-based shape memory alloys *Scr. Mater.* **135** 5–9
[18] Miyazaki S and Otsuka K 1989 Development of shape memory alloys *ISIJ Int.* **29** 353–77
[19] Chen Y and Schuh C A 2015 A coupled kinetic Monte Carlo–finite element mesoscale model for thermoelastic martensitic phase transformations in shape memory alloys *Acta Mater.* **83** 431–47
[20] Romero R and Pelegrina J L 2003 Change of entropy in the martensitic transformation and its dependence in Cu-based shape memory alloys *Mater. Sci. Eng.* A **354** 243–50
[21] Wang X, Jia Y, Yao Q, Wang F, Ma J and Hu X 2004 The calculation of the surface energy of high-index surfaces in metals at zero temperature *Surf. Sci.* **551** 179–88
[22] Pinhero P J, Anderegg J W, Sordelet D J, Besser M F and Thiel P A 1999 Surface oxidation of Al-Cu-Fe alloys: a comparison of quasicrystalline and crystalline phases *Phil. Mag.* B **79** 91–110
[23] Duerig T, Pelton A and Stöckel D 1999 An overview of Nitinol medical device applications *Mater. Sci. Eng.* A **273–275** 149–60
[24] Van Humbeeck J, Chandrasekaran M and Delaey L 1989 Influence of post quench ageing in the beta-phase on the transformation characteristics and the physical and mechanical properties of martensite in a Cu-Al-Ni shape memory alloy *ISIJ Int.* **29** 388–94
[25] Recarte V, Perez-Saez R B, Nó M L and San Juan J 1999 Ordering kinetics in Cu-Al-Ni shape memory alloys *J. Appl. Phys.* **86** 5467–73
[26] Pérez-Landazábal J I, Recarte V and Sánchez-Alarcos V 2005 Influence on the martensitic transformation of the β phase decomposition process in a Cu-Al-Ni shape memory alloy *J. Phys. Condens. Matter* **17** 4223–36